Faxén-like relations for a non-uniform suspension

Kengo Ichiki[1,*] and Andrea Prosperetti[1,2,†]

[1]*Department of Mechanical Engineering, The Johns Hopkins University, Baltimore MD 21218*
[2]*Faculty of Applied Physics, Twente Institute of Mechanics, and Burgerscentrum, University of Twente, AE 7500 Enschede, The Netherlands*

(Dated: March 12, 2004)

The first part of the paper shows how ensemble averages corresponding to a *prescribed* statistically non-uniform spatial distribution of particles can be evaluated starting from a statistically uniform ensemble. The method consists in attributing to each realization of the uniform ensemble a suitable weight which is explicitly constructed. As an application of this general procedure, in the second part of the paper, the behavior of particles subjected to a force or torque in a statistically non-uniform suspension, and the behavior of a suspension when subjected to a uniform shear, are studied. In particular, it is shown how the average translational and angular velocities of the particles with respect to the mixture satisfy Faxén-like relations. Furthermore, it is pointed out that several quantities which vanish identically in the case of a uniform suspension are non-zero in the presence of spatial non-uniformities.

I. INTRODUCTION

The construction of a general theory of suspensions and other disperse two-phase flows is an important problem in statistical physics and fluid mechanics, with significant implications for both science and technology.

In view of the limited success of phenomenological approaches, a considerable effort has been devoted to the development of such a theory starting from the fundamental microscopic description of the fluid-particle and particle-particle interactions. The early analytical studies by Batchelor,[1,2] Brenner,[3–5] Mazur,[6,7] and many others were mostly limited to dilute situations. The advent of powerful numerical simulation techniques, such as those described in Refs. 8–13, opened the way to the study of dense suspensions and the literature contains many papers devoted, on the one hand, to the characterization of dense suspensions in terms of their effective properties such as viscosity[14,15] and hindrance function[16] and, on the other, to the direct simulation of specific flows, such as channel flow.[17–19] In spite of the obvious usefulness of such direct simulations, computational limitations prevent their application to practical flows for which the only possible description is – and will remain for a long time to come – in terms of averaged equations. For this reason, the study of average effective properties such as effective viscosity and mean hydrodynamic interphase force remains of primary importance.

With very few exceptions restricted to the dilute situation,[20,21] all the studies devoted to the derivation of such macroscopic properties, dealt with statistically spatially uniform systems. It is clear that the view of suspension behavior gained in this way is a partial one. For example, in the simple shear flow of a uniform suspension, the velocity of force-free particles is the same as the local volumetric velocity of the mixture and, therefore, the only remaining effective property is the effective viscosity multiplying the rate-of-strain tensor of this mean flow. While, in principle, one could construct a rate-of-strain tensor of the relative motion and a corresponding viscosity,[22] no information on this new quantity can be gained from the simulation of a uniform system. The same remark applies to many other effective properties of a suspension. To be sure, formally, these non-uniformity effects scale as the ratio of the particle radius a to the macroscopic length L, or of the mean inter-particle distance $a\phi^{-1/3}$, where ϕ is the particle volume fraction, to L, but this consideration is not sufficient to dismiss them. For example while, in Stokes flow, the velocity disturbance generated by a particle extends over a distance proportional to a, the proportionality constant is large so that the corresponding a/L correction is not always negligible. Furthermore, important specific effects of spatial non-uniformity have been identified such as shear-induced diffusion,[23,24] stratification,[25,26] and others. Fundamentally, this issue is related to the finite size of the particles which is a central aspect of the behavior of dense suspensions.

These considerations have motivated our recent work on statistically non-homogeneous suspensions.[22,27–29] The present paper is a continuation and extension of that work and consists of two parts. In the first part, we show how ensemble averages corresponding to an *arbitrarily prescribed* macroscopic non-uniformity can be calculated. In the second part of the paper, we consider a simple such non-uniformity – a sine wave – and, by ensemble-averaging the results of many thousands of direct simulations, derive for a suspension Faxén-like relations analogous to the well-known ones applicable to single particles. It is also argued that, while the derivation of the result relies on a specific spatial non-uniformity, the validity of the conclusion is more general and extends to arbitrary situations with weak non-uniformities. Following a standard practice (see e.g. Ref. 10,15,30,31), the simulations are conducted in a periodic cell containing randomly arranged particles. The present formulation also confirms the earlier derivation of microscopic quantities, such as the mixture velocity, which was carried out by different means.[29]

In §II, we introduce an ensemble average method which

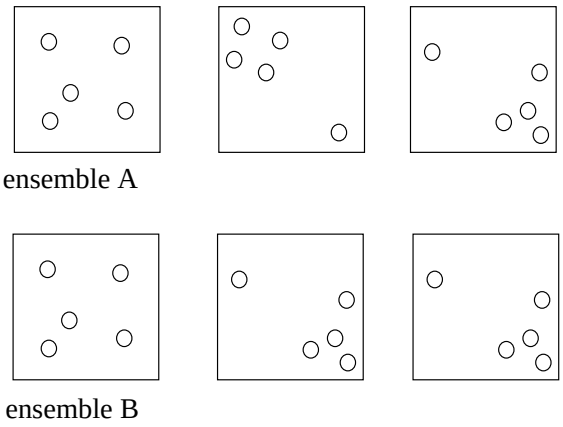

FIG. 1: A sketch of the generation of ensemble averages for spatially statistically non-uniform systems on the basis of a spatially uniform ensemble. Ensemble A is (roughly) uniform, while ensemble B has a preferential concentration of particles in the lower right corner. Averages over ensemble B can be calculated attributing weights of 1, 0, and 2, respectively, to the configurations of ensemble A.

can treat arbitrary non-uniformities. In §III, we show a procedure to evaluate physical quantities for non-uniform suspensions using the non-uniform ensemble average. In §V, the numerical results for a linear sinusoidal non-uniformity are shown.

II. NON-UNIFORM ENSEMBLE

A widely used procedure to study the bulk properties of an extended (ideally, infinite) suspension is to fill the space with copies of a fundamental cell in which the particles are randomly arranged. The relevant equations are then solved only in the fundamental cell with periodicity boundary conditions.

In this section, we demonstrate how to evaluate ensemble averages for a non-uniform suspension on the basis of a statistically uniform ensemble of random arrangements of particles inside the fundamental cell, thus avoiding the generation of an actual non-uniform ensemble. By this device, the uniform ensemble can be used to derive the statistical properties of a suspension with a built-in, prescribed, spatial non-uniformity.

A. Universal ensemble

By a procedure which will be explained below in Sec. IV C, we construct a statistical ensemble by randomly arranging N_p non-overlapping equal spherical particles with radius a in a cubic cell of side L.

In principle, this ensemble contains all possible configurations, regular and uniform as well as non-uniform or even heavily biased in the spatial arrangement of the particles. It is evident that, if an equal weight is assigned to each configuration, the resulting ensemble averages will correspond to a statistically homogeneous system. However, by giving the configurations unequal weights, this same ensemble can also mimic a spatially non-uniform system. It is for this reason that we refer to the ensemble thus constructed as "universal".

To illustrate the point by a simple cartoon-like example, Fig. 1 shows two ensembles A and B, each consisting of three configurations with 5 particles. ensemble A (roughly) describes a spatially uniform system, while ensemble B describes a system in which the accumulation of particles in the right lower corner is more likely. Evidently, instead of constructing the ensemble B, the same statistical bias can be obtained by assigning weights 1, 0 and 2, respectively, to the configurations in the ensemble A. This is obvious. The non-trivial question, to which we now provide an answer, is how to assign the weights in such a way that a *prescribed* spatial non-uniformity can be generated.

More precisely, in this section we consider the following problem: Given a generic quantity $A(\mathcal{C}_i^{N_p})$ pertaining to the i-th realization of an ensemble of N_c configurations $\{\mathcal{C}_1^{N_p}, \ldots, \mathcal{C}_{N_c}^{N_p}\}$, each one with N_p particles, define its average by

$$\langle A \rangle = \frac{1}{N_c} \sum_{i=1}^{N_c} \mathcal{W}(\mathcal{C}_i^{N_p})\ A(\mathcal{C}_i^{N_p})\,, \tag{1}$$

where the $\mathcal{W}(\mathcal{C}_i^{N_p})$'s are suitable weights. How should these weights be chosen for the average so defined to correspond to a system with a prescribed macroscopic non-uniformity in the particle position? Clearly, when all the weights are taken equal to 1, we have the uniform-ensemble average, denoted by the index 0:

$$\langle A \rangle_0 = \frac{1}{N_c} \sum_{i=1}^{N_c} A(\mathcal{C}_i^{N_p})\,. \tag{2}$$

B. Uniform and non-uniform averages

Each realization $\mathcal{C}_i^{N_p}$ of the ensemble consists of a set of vectors $\boldsymbol{x}_i^1, \boldsymbol{x}_i^2, \cdots, \boldsymbol{x}_i^{N_p}$ denoting the position of the center of particle $1, 2, \cdots, N_p$. For the realization $\mathcal{C}_i^{N_p} = \{\boldsymbol{x}_i^1, \boldsymbol{x}_i^2, \cdots, \boldsymbol{x}_i^{N_p}\}$, the (microscopic) number density is defined by

$$n_i(\boldsymbol{x}) = \sum_{\alpha=1}^{N_p} \delta\left(\boldsymbol{x} - \boldsymbol{x}_i^\alpha\right)\,, \tag{3}$$

and can be expanded in a Fourier series:

$$n_i(\boldsymbol{x}) = \sum_{\boldsymbol{k}} \tilde{n}_i(\boldsymbol{k}) e^{-i\boldsymbol{k}\cdot\boldsymbol{x}}\,, \tag{4}$$

with coefficients given by

$$\tilde{n}_i(\boldsymbol{k}) = \frac{1}{V}\int d\boldsymbol{x}\; e^{i\boldsymbol{k}\cdot\boldsymbol{x}} n_i(\boldsymbol{x}) \;=\; \frac{1}{V}\sum_{\alpha=1}^{N_p} e^{i\boldsymbol{k}\cdot\boldsymbol{x}_i^\alpha}, \quad (5)$$

where $V = L^3$ is the volume of the fundamental cell. The summation in (4) is extended to all the vectors $\boldsymbol{k}$ compatible with the cell. For $\boldsymbol{k} = \boldsymbol{0}$ we evidently have

$$\tilde{n}_i(\boldsymbol{0}) \;=\; \frac{N_p}{V} \;=\; n_0 \quad (6)$$

for all realizations and, therefore,

$$\langle n\rangle_0 = n_0\,, \quad (7)$$

the volume-averaged particle number density. For non-zero $\boldsymbol{k}$, we have

$$\langle\tilde{n}(\boldsymbol{k})\rangle_0 = \langle\frac{1}{V}\sum_{\alpha=1}^{N_p} e^{i\boldsymbol{k}\cdot\boldsymbol{x}_i^\alpha}\rangle_0 = 0. \quad (8)$$

Thus, we may write

$$\langle\tilde{n}(\boldsymbol{k})\rangle_0 = n_0\delta_{\boldsymbol{k}0}. \quad (9)$$

For $\boldsymbol{k}\neq 0$, the static structure factor $S(\boldsymbol{k})$ of the uniform ensemble is related to $\tilde{n}$ by

$$\langle\tilde{n}(-\boldsymbol{k}')\;\tilde{n}(\boldsymbol{k})\rangle_0 = \delta_{\boldsymbol{k}'\boldsymbol{k}}\frac{N_p}{V^2}S(\boldsymbol{k}). \quad (10)$$

In order to generate weights for the non-uniform ensemble, we introduce a function $w(\boldsymbol{x})$ regular in the fundamental cell and with the same periodicity, and assign to the i-th realization $\mathcal{C}_i^{N_p}$ the weight $\mathcal{W}(\mathcal{C}_i^{N_p})$ defined by

$$\begin{aligned}\mathcal{W}(\mathcal{C}_i^{N_p}) \;&=\; \frac{1}{N_p}\sum_{\alpha=1}^{N_p} w(\boldsymbol{x}_i^\alpha) = \frac{1}{N_p}\int d\boldsymbol{x}\, w(\boldsymbol{x})\, n_i(\boldsymbol{x}) \\ &=\; \frac{1}{n_0}\sum_{\boldsymbol{k}}\tilde{w}(\boldsymbol{k})\;\tilde{n}_i(-\boldsymbol{k}). \end{aligned} \quad (11)$$

The relation between the function $w(\boldsymbol{x})$ and the spatial structure of the ensemble is readily found by calculating the average number density with the above-defined weights. For $\boldsymbol{k} = \boldsymbol{0}$ we have

$$\langle\tilde{n}(\boldsymbol{0})\rangle = n_0\frac{V}{N_p}\sum_{\boldsymbol{k}}\tilde{w}(\boldsymbol{k})\langle\tilde{n}(-\boldsymbol{k})\rangle_0 = n_0\tilde{w}(\boldsymbol{0}), \quad (12)$$

where we use (1) with (6) and (11), from which $\tilde{w}(\boldsymbol{0}) = 1$. For $\boldsymbol{k}\neq\boldsymbol{0}$,

$$\begin{aligned}\langle\tilde{n}(\boldsymbol{k})\rangle \;&=\; \frac{1}{N_c}\sum_{i=1}^{N_c}\mathcal{W}(\mathcal{C}_i^{N_p})\;\tilde{n}_i(\boldsymbol{k}) \\ &=\; \tilde{w}(\boldsymbol{k})\frac{S(\boldsymbol{k})}{V}, \end{aligned} \quad (13)$$

where we use (10). We thus conclude that, if the desired average number density is given by

$$\langle n\rangle(\boldsymbol{x}) \equiv n(\boldsymbol{x}), \quad (14)$$

we can generate it by assigning to each configuration of the ensemble a weight according to (11), where the function w is given in terms of its Fourier coefficients by

$$\tilde{w}(\boldsymbol{k}) = \frac{V}{S(\boldsymbol{k})}\tilde{n}(\boldsymbol{k}), \quad (15)$$

in which $\tilde{n}(\boldsymbol{k})$ is the Fourier coefficient of the prescribed number density (14).

C. Field and particle quantities

Extending the previous considerations to a generic field quantity $A(\boldsymbol{x})$, we expand it in a Fourier series as

$$A(\boldsymbol{x}) = \sum_{\boldsymbol{k}}\tilde{A}(\boldsymbol{k})e^{-i\boldsymbol{k}\cdot\boldsymbol{x}}\,, \quad (16)$$

where

$$\tilde{A}(\boldsymbol{k}) = \frac{1}{V}\int d\boldsymbol{x}\; e^{i\boldsymbol{k}\cdot\boldsymbol{x}}A(\boldsymbol{x}). \quad (17)$$

The non-uniform ensemble average of A with the weight $\tilde{w}(\boldsymbol{k})$ is given by

$$\begin{aligned}&\langle A\rangle(\boldsymbol{x}) = \langle\tilde{A}(\boldsymbol{0})\rangle_0 \\ &+\frac{1}{n_0}\sum_{\boldsymbol{k}\neq\boldsymbol{0}}\sum_{\boldsymbol{k}'}\tilde{w}(\boldsymbol{k}')\langle\tilde{n}(-\boldsymbol{k}')\;\tilde{A}(\boldsymbol{k})\rangle_0\; e^{-i\boldsymbol{k}\cdot\boldsymbol{x}}, \end{aligned} \quad (18)$$

where the averages carrying the subscript 0 are taken over the homogeneous ensemble as defined in (2). This form is found after observing that, for $\boldsymbol{k}\neq 0$, $\langle\tilde{n}(-\boldsymbol{k})\;\tilde{A}(\boldsymbol{0})\rangle_0 = 0$ and $\langle\tilde{A}(\boldsymbol{k})\rangle_0 = 0$.

Rather than dealing with complex exponentials, for actual computations it is more convenient to make use of Fourier expansions in real form. For a generic field quantity $A(\boldsymbol{x})$ the Fourier representation analogous to (16) is

$$A(\boldsymbol{x}) = \tilde{A}(\boldsymbol{0}) + \sum_{\boldsymbol{k}>0}\Big\{\tilde{A}^c(\boldsymbol{k})\cos(\boldsymbol{k}\cdot\boldsymbol{x}) + \tilde{A}^s(\boldsymbol{k})\sin(\boldsymbol{k}\cdot\boldsymbol{x})\Big\}, \quad (19)$$

where the symbol $\boldsymbol{k}>0$ appended to the summation restricts it to wave numbers all the components of which are positive, and

$$\tilde{A}^c(\boldsymbol{k}) \;=\; \frac{2}{V}\int d\boldsymbol{x}\; A(\boldsymbol{x})\cos(\boldsymbol{k}\cdot\boldsymbol{x})\,, \quad (20)$$

$$\tilde{A}^s(\boldsymbol{k}) \;=\; \frac{2}{V}\int d\boldsymbol{x}\; A(\boldsymbol{x})\sin(\boldsymbol{k}\cdot\boldsymbol{x})\,. \quad (21)$$

In addition to field variables, the averages of quantities A^α carried by each particle α are also of interest. Examples are the translational and angular velocity, the force

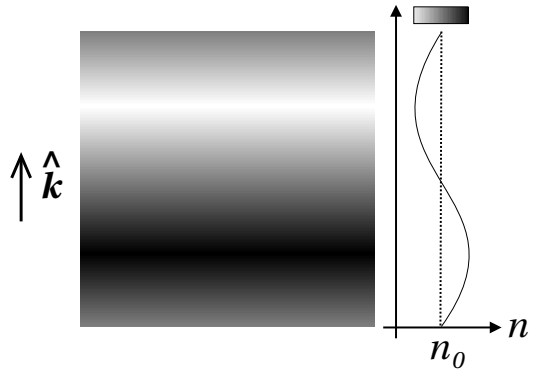

FIG. 2: An example of the linear sinusoidal non-uniformity.

multipoles, and others. In order to calculate these averages, we first transform A^α to a field variable by writing

$$A(\boldsymbol{x}) = \sum_{\alpha=1}^{N_p} \delta\left(\boldsymbol{x} - \boldsymbol{x}^\alpha\right) A^\alpha. \tag{22}$$

The Fourier coefficients are then

$$\tilde{A}^c(\boldsymbol{k}) \;=\; \frac{2}{V}\sum_{\alpha=1}^{N_p} A^\alpha \cos\left(\boldsymbol{k}\cdot\boldsymbol{x}^\alpha\right), \tag{23}$$

$$\tilde{A}^s(\boldsymbol{k}) \;=\; =\frac{2}{V}\sum_{\alpha=1}^{N_p} A^\alpha \sin\left(\boldsymbol{k}\cdot\boldsymbol{x}^\alpha\right), \tag{24}$$

and their averages are readily calculated by summing over the configurations as in (18). After this step, the particle average is calculated from

$$\langle A\rangle^P(\boldsymbol{x}) = \frac{\langle A\rangle(\boldsymbol{x})}{\langle n\rangle(\boldsymbol{x})}. \tag{25}$$

The need for the normalization by $\langle n\rangle(\boldsymbol{x})$ is readily proven by considering the special case $A^\alpha = 1$. By this device, we can treat in a unified way both field and particle quantities through their Fourier coefficients $\tilde{A}(\boldsymbol{k})$.

D. Linear sinusoidal non-uniformity

In the applications of the statistical method to be described in this paper, we limit ourselves to a non-uniform suspension with a weak spatial nonuniformity specified by the number density

$$n(\boldsymbol{x}) = n_0\left(1 + \epsilon\sin\left(\boldsymbol{k}\cdot\boldsymbol{x}\right)\right). \tag{26}$$

It will be argued, however, that the results found in this way extend to general weak non-uniformities. In (26) we take $|\boldsymbol{k}|$ equal in modulus to the smallest wave number $k_0 = 2\pi/L$ and oriented in one of the three spatial directions. Henceforth, the symbol $\boldsymbol{k}$ will denote one of these three wave-number vectors. The parameter ϵ is the degree of non-uniformity, and we present results valid to the first order in this quantity. In principle, since the Stokes problem that we study is linear, linearization in ϵ enables us to use Fourier superposition to describe weak non-uniformities of any form. It may be noted that, to first order in k included, the volume fraction ϕ has the same spatial dependence[27]

$$\phi(\boldsymbol{x}) \;=\; \phi_0\,\left(1 + \epsilon\,\sin\left(\boldsymbol{k}\cdot\boldsymbol{x}\right)\right) + O(k^2)\,, \tag{27}$$

in which $\phi_0 = \frac{4}{3}\pi a^3 n_0$.

With this choice of $n(\boldsymbol{x})$, all the weight coefficients vanish except

$$\tilde{w}(\boldsymbol{0}) = 1, \quad \tilde{w}^s(\boldsymbol{k}) = \epsilon n_0 \frac{V}{S(\boldsymbol{k})}. \tag{28}$$

Therefore, the non-uniform ensemble average of a the Fourier coefficients $\tilde{A}$ becomes

$$\langle\tilde{A}\rangle = \langle\tilde{A}\rangle_0 + \epsilon\langle\tilde{A}\rangle_s, \tag{29}$$

where the non-uniform part $\langle\tilde{A}\rangle_s$ is given by

$$\langle\tilde{A}\rangle_s = \frac{1}{2}\frac{V}{S(k)}\langle\tilde{n}^s(\boldsymbol{k})\;\tilde{A}\rangle_0, \tag{30}$$

with, on the basis of (5),

$$\tilde{n}^s(\boldsymbol{k}) = \frac{2}{V}\sum_{\alpha=1}^{N_p}\sin\left(\boldsymbol{k}\cdot\boldsymbol{x}^\alpha\right)\,. \tag{31}$$

The ensemble average of the Fourier expansion (19) therefore takes the form

$$\langle A\rangle(\boldsymbol{x}) = \langle\tilde{A}(\boldsymbol{0})\rangle_0 + \epsilon\left[\langle\tilde{A}^c(\boldsymbol{k})\rangle_s\cos\left(\boldsymbol{k}\cdot\boldsymbol{x}\right) + \langle\tilde{A}^s(\boldsymbol{k})\rangle_s\sin\left(\boldsymbol{k}\cdot\boldsymbol{x}\right)\right], \tag{32}$$

since all other coefficients vanish.

For particle averages, (25) gives, up to $O(\epsilon)$,

$$\langle A\rangle^P(\boldsymbol{x}) = \frac{1}{n_0}\left\{\langle\tilde{A}(\boldsymbol{0})\rangle_0 + \epsilon\left[\langle\tilde{A}^c(\boldsymbol{k})\rangle_s\cos\left(\boldsymbol{k}\cdot\boldsymbol{x}\right) + \left(\langle\tilde{A}^s(\boldsymbol{k})\rangle_s - \langle\tilde{A}(\boldsymbol{0})\rangle_0\right)\sin\left(\boldsymbol{k}\cdot\boldsymbol{x}\right)\right]\right\}. \tag{33}$$

Equations (32) and (33) show another reason why the introduction of the parameter ϵ is useful: the terms multiplied by ϵ originate exclusively from the spatial nonuniformity and, therefore, by focusing on them, we are able to identify unambiguously the effect of this nonuniformity even in the presence of the inevitable statistical noise.

III. PARAMETERIZATION

In this paper, we study three kinds of mobility problems for non-uniform suspensions, namely the flow induced by mobile particles subject to a constant force (referred to as "force problem" in the following), a constant

torque ("torque problem"), or a shear bulk flow ("shear problem"). We carry out direct numerical simulations by solving the Stokes equations for each configuration of the ensemble by the method described later in Sec IV. From the results for each realization of the ensemble, we calculate statistical averages according to the relations developed in the previous section.

It is useful to present the results using a suitable parameterization, which we now describe. For convenience, we make use of a unified notation which is first introduced in the context of the force problem, and then extended to the other cases.

A. Force problem

For the force problem, i.e., sedimentation, we conduct numerical simulations where the same force $\boldsymbol{F}_0$ is applied to each particle. The uniform version of this problem is therefore characterized by a single fundamental vector

$$\boldsymbol{W}_F \;=\; \frac{\boldsymbol{F}_0}{6\pi\mu a} \tag{34}$$

with μ the fluid viscosity, and, therefore, any vectorial dependent variable $\boldsymbol{p}$, such as the mean settling velocity, must take the form

$$\langle \boldsymbol{p} \rangle = [p]^0_F \, \boldsymbol{W}_F, \tag{35}$$

where $[p]^0_F$ is a coefficient calculated numerically by taking the ensemble average of the values of $\boldsymbol{p}$. Here and in the following we use the subscript F for all quantities which refer to the applied force problem.

When we turn to the non-uniform case, in addition to $\boldsymbol{W}_F$, also the wave vector $\boldsymbol{k}$ specifying the direction of the non-uniformity is introduced. Therefore, it must be possible to parameterize the non-uniform part of each vectorial dependent variable as

$$\langle \boldsymbol{p} \rangle = [p]^{\parallel}_F \, \boldsymbol{W}^{\parallel}_F + [p]^{\perp}_F \, \boldsymbol{W}^{\perp}_F, \tag{36}$$

where the superscripts $\parallel$ and $\perp$ are based on the direction of the unit wave vector $\hat{\boldsymbol{k}}$ and

$$\boldsymbol{W}^{\parallel}_F \;=\; \left(\hat{\boldsymbol{k}}\hat{\boldsymbol{k}}\right) \cdot \boldsymbol{W}_F, \tag{37}$$

$$\boldsymbol{W}^{\perp}_F \;=\; \left(\mathsf{I} - \hat{\boldsymbol{k}}\hat{\boldsymbol{k}}\right) \cdot \boldsymbol{W}_F. \tag{38}$$

Clearly $\boldsymbol{W}_F = \boldsymbol{W}^{\parallel}_F + \boldsymbol{W}^{\perp}_F$. The only characteristic pseudo-vector is

$$a\boldsymbol{\omega}^{\perp}_F \;=\; \hat{\boldsymbol{k}} \times \boldsymbol{W}_F, \tag{39}$$

which is perpendicular to $\boldsymbol{k}$; the factor a is included so that $\boldsymbol{\omega}^{\perp}_F$ has the dimensions of an angular velocity. Therefore, any pseudo vector $\boldsymbol{q}$ must be parameterized as

$$\boldsymbol{q} = [q]^{\perp}_F \, \boldsymbol{\omega}^{\perp}_F. \tag{40}$$

Note that $a\hat{\boldsymbol{k}} \times \boldsymbol{\omega}^{\perp}_F = -\boldsymbol{W}^{\perp}_F$, and the parallel component $\boldsymbol{\omega}^{\parallel}_F$ is zero.

B. Torque problem

In the second problem, we apply a constant torque $\boldsymbol{T}_0$ to each particle and use the subscript T to denote the pertaining quantities. Here, for the uniform case, pseudo vectors must be parameterized as

$$\boldsymbol{q} = [q]^0_T \, \boldsymbol{\omega}_T, \tag{41}$$

with

$$\boldsymbol{\omega}_T = \frac{\boldsymbol{T}_0}{8\pi\mu a^3}. \tag{42}$$

For the non-uniform case we have a single vector:

$$\boldsymbol{W}^{\perp}_T = a\hat{\boldsymbol{k}} \times \boldsymbol{\omega}_T, \tag{43}$$

and two pseudo vectors:

$$\boldsymbol{\omega}^{\parallel}_T \;=\; \left(\hat{\boldsymbol{k}} \cdot \boldsymbol{\omega}_T\right) \hat{\boldsymbol{k}}, \tag{44}$$

$$\boldsymbol{\omega}^{\perp}_T \;=\; \left(\mathsf{I} - \hat{\boldsymbol{k}}\hat{\boldsymbol{k}}\right) \cdot \boldsymbol{\omega}_T. \tag{45}$$

Note that $\hat{\boldsymbol{k}} \times \boldsymbol{W}^{\perp}_T = -a\boldsymbol{\omega}^{\perp}_T$.

C. Shear problem

In the third problem, we apply a linear shear flow, so that, even in the uniform case, there is an imposed velocity field given by

$$\boldsymbol{u}^{\infty}(\boldsymbol{x}) \;=\; \mathsf{E}^{\infty} \cdot \boldsymbol{x}. \tag{46}$$

where E^{∞} is the rate-of-strain tensor of the flow and is symmetric and traceless. The corresponding results will carry an index E. Because we cannot construct any vector or pseudo vector from E^{∞} only, there cannot be any uniform contribution to vectors $\boldsymbol{a}$ or pseudo-vectors $\boldsymbol{b}$ for the shear problem. In the non-uniform case, one can construct two characteristic vectors:

$$\boldsymbol{W}^{\parallel}_E \;=\; a\left(\hat{\boldsymbol{k}}\hat{\boldsymbol{k}}\right) \cdot \left(\mathsf{E}^{\infty} \cdot \hat{\boldsymbol{k}}\right), \tag{47}$$

$$\boldsymbol{W}^{\perp}_E \;=\; a\left(\mathsf{I} - \hat{\boldsymbol{k}}\hat{\boldsymbol{k}}\right) \cdot \left(\mathsf{E}^{\infty} \cdot \hat{\boldsymbol{k}}\right), \tag{48}$$

and one characteristic pseudo vector

$$\boldsymbol{\omega}^{\perp}_E \;=\; \hat{\boldsymbol{k}} \times \left(\mathsf{E}^{\infty} \cdot \hat{\boldsymbol{k}}\right). \tag{49}$$

Note that $a\,\hat{\boldsymbol{k}} \times \boldsymbol{\omega}^{\perp}_E = -\boldsymbol{W}^{\perp}_E$.

D. Summary

Because of the linearity of the Stokes flow, the results for these three problems can be superposed. Therefore,

vectors $\langle \boldsymbol{p} \rangle$ and pseudo-vectors $\langle \boldsymbol{q} \rangle$ are generally parameterized as

$$\begin{aligned} \langle \boldsymbol{p} \rangle &= [p]^0_F \, \boldsymbol{W}_F \\ &+ [p]^{\parallel}_F \, \boldsymbol{W}^{\parallel}_F + [p]^{\perp}_F \, \boldsymbol{W}^{\perp}_F \\ &+ [p]^{\perp}_T \, \boldsymbol{W}^{\perp}_T \\ &+ [p]^{\parallel}_E \, \boldsymbol{W}^{\parallel}_E + [p]^{\perp}_E \, \boldsymbol{W}^{\perp}_E, \end{aligned} \tag{50}$$

and

$$\begin{aligned} \langle \boldsymbol{q} \rangle &= [q]^0_T \, \boldsymbol{\omega}_T \\ &+ [q]^{\perp}_F \, \boldsymbol{\omega}^{\perp}_F \\ &+ [q]^{\parallel}_T \, \boldsymbol{\omega}^{\parallel}_T + [q]^{\perp}_T \, \boldsymbol{\omega}^{\perp}_T \\ &+ [q]^{\perp}_E \, \boldsymbol{\omega}^{\perp}_E. \end{aligned} \tag{51}$$

IV. NUMERICAL METHOD

We now introduce suitable expressions for the quantities on which we focus in this paper, namely the average mixture velocity (or volumetric flux), denoted by $\langle \boldsymbol{u}_m \rangle$, the average mixture angular velocity, $\langle \boldsymbol{\Omega}_m \rangle$, the average particle velocity, $\langle \boldsymbol{U} \rangle$, and the average particle angular velocity $\langle \boldsymbol{\Omega} \rangle$. The numerical procedures developed in the previous sections and applied to the above quantities are also outlined. The results will be shown and discussed in the next section.

A. Many-body problem

The input to the non-uniform ensemble averaging procedure is the solution of the Stokes many-body problem, which can be expressed in the form of a generalized mobility equation,

$$\begin{bmatrix} \boldsymbol{U} - \boldsymbol{U}^{\infty} \\ \boldsymbol{\Omega} - \boldsymbol{\Omega}^{\infty} \\ -\mathsf{E}^{\infty} \\ -\mathscr{U}^{\infty} \end{bmatrix} = \mathcal{M} \cdot \begin{bmatrix} \boldsymbol{F} \\ \boldsymbol{T} \\ \mathsf{S} \\ \mathscr{F} \end{bmatrix}, \tag{52}$$

where $\boldsymbol{U}$, $\boldsymbol{\Omega}$ are translational and rotational velocities of the particles, and $\boldsymbol{U}^{\infty}$ and $\boldsymbol{\Omega}^{\infty}$ are defined by

$$\boldsymbol{U}^{\infty}(\alpha) = \frac{1}{4\pi a^2} \int_{S^{\alpha}} dS(\boldsymbol{y}) \; \boldsymbol{u}^{\infty}, \tag{53}$$

$$\boldsymbol{\Omega}^{\infty}(\alpha) = \frac{1}{4\pi a^2} \int_{S^{\alpha}} dS(\boldsymbol{y}) \; \frac{3}{2a^2} \, (\boldsymbol{y} - \boldsymbol{x}^{\alpha}) \times \boldsymbol{u}^{\infty}(\boldsymbol{y}) \tag{54}$$

Furthermore, E^{∞}, and $\mathscr{U}^{\infty}$ are the strain tensor and higher order velocity moments, of the imposed flow $\boldsymbol{u}^{\infty}$, $\mathcal{M}$ is the generalized mobility matrix, and $\boldsymbol{F}$, $\boldsymbol{T}$, S, and $\mathscr{F}$ are force, torque, stresslet, and higher order force moments of the particles.[8,32] Detailed definitions are summarized in Appendix A. When $\boldsymbol{u}^{\infty}$ is itself a Stokes velocity field and, therefore, biharmonic, we have

$$\boldsymbol{U}^{\infty}(\alpha) = \left(1 + \frac{a^2}{6} \nabla^2\right) \boldsymbol{u}^{\infty}(\boldsymbol{x}^{\alpha}), \tag{55}$$

$$\boldsymbol{\Omega}^{\infty}(\alpha) = \frac{1}{2} \boldsymbol{\nabla} \times \boldsymbol{u}^{\infty}(\boldsymbol{x}^{\alpha}). \tag{56}$$

The three problems we study are mobility problems, so that $\boldsymbol{F}$ and $\boldsymbol{T}$ are prescribed. For the imposed flow problem, the quantities $\boldsymbol{U}^{\infty}$, $\boldsymbol{\Omega}^{\infty}$, E^{∞}, and $\mathscr{U}^{\infty}$ are also given. Therefore, (52) can be solved, and we obtain $\boldsymbol{U}$, $\boldsymbol{\Omega}$, S, and $\mathscr{F}$ for each configuration.

To solve the many-body problem, we use the same numerical code as in the previous papers,[22,27] which is based on the method developed by Mo and Sangani.[31] This step is the most time-consuming part of the present method. In the code, $\mathscr{F}$ is expressed by the coefficients of spherical harmonics appearing in Lamb's general solution.[33,34] In order to save time, we use the solutions of the many-body problems obtained in Refs. 22,27, to which we add new calculations for many other values of both volume fraction ϕ and particle number N_p. For consistency we use the same parameters, taking into account multipoles up to the fifth order. In the final processing of the data, however, only multipoles up to the fourth order are included.

For several cases, we also used the Stokesian Dynamics method[32] extended to a periodic system (see Appendix A), and have confirmed that the two methods give the same results within the accuracy of the multipole truncation.

B. Mixture velocity

Besides the particle quantities such as $\boldsymbol{U}$ and $\boldsymbol{\Omega}$, we are also interested in $\boldsymbol{u}_m$, the volumetric flux of the mixture. Tanksley and Prosperetti[29] give a detailed expression of $\boldsymbol{u}_m$ in terms of Lamb's coefficients, Here, we give another expression of $\boldsymbol{u}_m$.

For a single realization of the ensemble, the mixture velocity $\boldsymbol{u}_m$ is given by the integral[35,36]

$$\boldsymbol{u}_m(\boldsymbol{x}) - \boldsymbol{u}^{\infty}(\boldsymbol{x}) = -\frac{1}{8\pi\mu} \sum_{\alpha=1}^{N_p} \int_{S^{\alpha}} dS(\boldsymbol{y}) \; \mathsf{J}(\boldsymbol{x} - \boldsymbol{y}) \cdot \boldsymbol{f}(\boldsymbol{y}), \tag{57}$$

where $\boldsymbol{u}^{\infty}$ is the imposed flow, J is the Green function of the problem, and $\boldsymbol{f}$ is the force density at position $\boldsymbol{y}$ on the surface of the α-th particle.

Note that the $\boldsymbol{u}_m$ given by (57) is not only defined in the fluid domain, but also inside the particles, where, in fact, it is identical to the rigid-body value

$$\boldsymbol{u}_m(\boldsymbol{x}) = \boldsymbol{U}^{\alpha} + \boldsymbol{\Omega}^{\alpha} \times \boldsymbol{x}, \tag{58}$$

because it is the Stokes solution satisfying this equation on the particle surface due to the no-slip condition. Therefore, (57) not only gives the fluid velocity in the

fluid domain, but also the volumetric flux of the mixture in the whole domain.

In the present theory, we need the Fourier coefficients of the mixture velocity rather than $\boldsymbol{u}_m(\boldsymbol{x})$ itself. In this case, we can avoid the complexity of the Ewald summation for periodic boundary conditions and use the expression valid in an infinite volume by modifying the wave vector $\boldsymbol{k}$ from a continuous to a discrete variable; $\mathsf{J}(\boldsymbol{r})$ is then the Oseen tensor given by

$$\mathsf{J}(\boldsymbol{r}) = \frac{1}{r}\left(\mathsf{I} + \frac{\boldsymbol{r}\boldsymbol{r}}{r^2}\right). \tag{59}$$

This is the same procedure for the analysis of a periodic system used by Ladd[10] and applied to an infinite system in Ref. 7. Upon using the convolution relation in (57), the Fourier coefficient of the relative velocity $(\boldsymbol{u}_m - \boldsymbol{u}^\infty)$ is given by

$$\left(\tilde{u}_m\right)_i(\boldsymbol{k}) = \frac{1}{\mu}\frac{1}{k^2}\left(\delta_{ij} - \frac{k_i k_j}{k^2}\right)\sum_{n=0}^{\infty}\frac{i^n k_{k\cdots}^n}{n!}\tilde{\mathscr{F}}^{(n)}_{j,k\cdots}(\boldsymbol{k}), \tag{60}$$

where $\tilde{\mathscr{F}}(\boldsymbol{k})$ is the Fourier coefficient of the force moment $\mathscr{F}$. In real form, the cosine and sine coefficients are

$$\left(\tilde{u}^c_m\right)_i(\boldsymbol{k}) = \frac{1}{\mu}\frac{1}{k^2}\left(\delta_{ij} - \frac{k_i k_j}{k^2}\right)\sum_{n=0}^{\infty}(-)^n\left[\frac{k_{k\cdots}^{2n}}{(2n)!}\tilde{\mathscr{F}}^{c(2n)}_{j,k\cdots}(\boldsymbol{k}) - \frac{k_{k\cdots}^{2n+1}}{(2n+1)!}\tilde{\mathscr{F}}^{s(2n+1)}_{j,k\cdots}(\boldsymbol{k})\right], \tag{61}$$

$$\left(\tilde{u}^s_m\right)_i(\boldsymbol{k}) = \frac{1}{\mu}\frac{1}{k^2}\left(\delta_{ij} - \frac{k_i k_j}{k^2}\right)\sum_{n=0}^{\infty}(-)^n\left[\frac{k_{k\cdots}^{2n}}{(2n)!}\tilde{\mathscr{F}}^{s(2n)}_{j,k\cdots}(\boldsymbol{k}) + \frac{k_{k\cdots}^{2n+1}}{(2n+1)!}\tilde{\mathscr{F}}^{c(2n+1)}_{j,k\cdots}(\boldsymbol{k})\right], \tag{62}$$

where $\tilde{\mathscr{F}}^c(\boldsymbol{k})$ and $\tilde{\mathscr{F}}^s(\boldsymbol{k})$ are the cosine and sine coefficients of the force moment. Equation (60) is equivalent to (8.2) in the paper by Tanksley and Prosperetti.[29]

Note that the coefficient with $\boldsymbol{k} = \boldsymbol{0}$ should be dropped in order for the velocity to be non-singular.[30,37] This specifies the frame of reference as the volume average of the mixture velocity in the fundamental cell is then zero. This is the physical meaning of Batchelor's renormalization.[1]

C. Ensembles

Our interest lies in quantities corresponding to large (ideally infinite) systems, for which $k \to 0$. For each value of ϕ, therefore, it is necessary to construct ensembles corresponding to different values of k so as to be able to calculate this limit. This requires the consideration of ensembles with different number of particles N_p as

$$ka = \frac{2\pi a}{L} = \left(\frac{6\pi^2\phi}{N_p}\right)^{1/3}. \tag{63}$$

TABLE I: Number of configurations in the ensemble used in the simulations.

number of particles N_p	number of configurations N_c
10 – 16	2048
17 – 79	1024
80 – 150	512
160	256

For ϕ between 1 and 50%, we construct ensembles of between 256 and 2048 configurations with 10 to 160 particles. Statistical errors in the ensemble averages (2) decrease rather slowly as $1/\sqrt{N_c}$. Considerations of computational time force us to strike a compromise between number of configurations and residual statistical error, especially for large numbers of particles. Table I shows the numbers of configurations we use in the different ensembles.

The ensembles are constructed as follows. For volume fractions less than 50%, we start by randomly arranging the particles in the cell making sure that no overlap occurs, and subject them to a random walk displacing each one of them taking care to avoid overlaps at each step. After $100N_p$ steps per particle, we store the resultant configuration as a member of the ensemble. The initial configuration is regenerated every time. For $\phi = 50\%$, we start by arranging the N_p particles in a regular array and execute $1000N_p$ random steps after which we store the resulting configuration. This configuration is used as the starting condition for generating the next one. By repeating this procedure, we construct ensembles of N_c configurations.

The static structure factor for hard-spheres in infinite space is isotropic and is approximated by the analytical solution of the Percus-Yevick integral equation[38–40] as

$$S_{PY}(k) = \left(1 - n_0\tilde{c}(2ka)\right)^{-1}, \tag{64}$$

where n_0 is the number density, and $\tilde{c}(2ka)$ is the Fourier transform of the direct (isotropic) correlation function

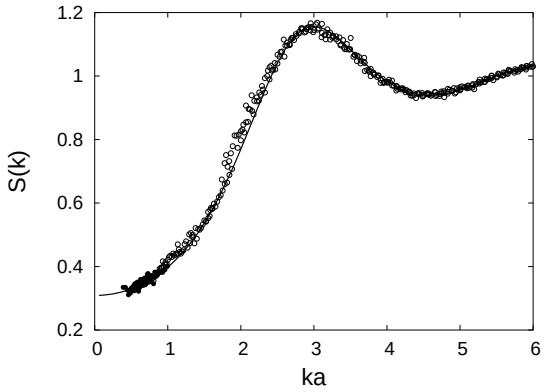

FIG. 3: Comparison between the structure factor given by the Percus-Yevick solution $S_{PY}(k)$ in (64) (solid line) and $S(k)$ numerically calculated from (69) from the configurations used in the present work for $\phi = 0.15$. The solid circles are calculated with $k = 2\pi/L$, and the open circles are with higher spatial modes.

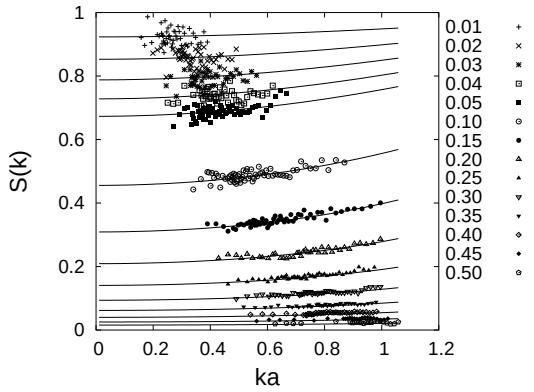

FIG. 4: The structure factor $S_s(k)$ calculated according to (70) for the smallest wave number for each cell for all ensembles used in this study with volume fraction ϕ between 0.01 and 0.50 and particle number N_p between 10 and 160. The lines are the Percus-Yevick solution $S_{PY}(k)$ in (64) for each volume fraction.

given by

$$\begin{aligned}\tilde{c}(X) &= -\frac{32\pi a^3}{X^3}\left[\alpha\left(\sin X - X\cos X\right)\right.\\ &\quad +\frac{\beta}{X}\left\{2X\sin X - (X^2-2)\cos X - 2\right\}\\ &\quad +\frac{\gamma}{X^3}\left\{\left(4X^3-24X\right)\sin X\right.\\ &\quad \left.\left.-\left(X^4-12X^2+24\right)\cos X + 24\right\}\right], \qquad (65)\end{aligned}$$

where $X = 2ka$, and

$$\alpha(\phi) = \frac{(1+2\phi)^2}{(1-\phi)^4}, \qquad (66)$$

$$\beta(\phi) = -6\phi\frac{(1+\frac{1}{2}\phi)^2}{(1-\phi)^4}, \qquad (67)$$

$$\gamma(\phi) = \frac{\phi}{2}\frac{(1+2\phi)^2}{(1-\phi)^4}. \qquad (68)$$

Figure 3 shows a comparison between $S_{PY}(k)$ and the structure factor $S(k)$ for our ensembles for a volume fraction of 15%. We calculate this quantity according to

$$S(k) = \frac{V^2}{N_p}\langle\tilde{n}(\boldsymbol{k})\tilde{n}(-\boldsymbol{k})\rangle_0, \qquad (69)$$

considering not only $k = 2\pi/L$, but also the higher modes $\sqrt{2}k$, $\sqrt{3}k$, $2k$, and so on. For each wave vector, the point plotted in Fig. 3 is the average over all the different directions of the wave vector. This result shows that, although our ensembles are not strictly isotropic, they give rise to a structure factor essentially indistinguishable from the Percus-Yevick distribution in infinite space in the wave vectors range greater than $2\pi/L$. In particular, one may therefore expect that the linear sinusoidal non-uniformity with the smallest wave number k is not affected by the periodicity.

For all our ensembles, Fig. 4 shows the unscaled non-uniform averages of $\tilde{n}^s(\boldsymbol{k})$ for the case of a linear sinusoidal non-uniformity. According to (30), this quantity is defined by

$$S_s(k) = \frac{V^2}{2N_p}\langle(\tilde{n}^s(\boldsymbol{k}))^2\rangle_0. \qquad (70)$$

Every point represents an ensemble average for given values of ϕ and N_p. A comparison of this figure with Fig. 3 in the previous paper[27], shows that, while some results for volume fractions $\phi = 0.15$, 0.25, and 0.35 have been reused as mentioned before, many more ensembles have been added since then. Note that the universal ensemble is translationally invariant, so that the average $\langle(\tilde{n}^c)^2\rangle_0$ is equal to $\langle(\tilde{n}^s)^2\rangle_0$ within the statistical accuracy. Therefore, $S_s(k)$ in (70) is equal to $S(k)$ in (69). In the figure, we also plot $S_{PY}(k)$ as a reference. This shows that the relative error of $S_s(k)$ from $S_{PY}(k)$ is independent of ϕ and around 6 to 8 %.

In the calculations that follow, we use this numerically computed $S_s(k)$ as the structure factor in the definition of the non-uniform probability weights in (28).

D. Averaging and parameterization

Here we show how to evaluate the non-uniform ensemble averages with the universal ensembles for each one of the quantities defined above.

1. Field quantities

The Fourier coefficients of the mixture velocity defined by (61) and (62) are averaged according to (29) for each ensemble. Since the coefficient with $\boldsymbol{k} = \boldsymbol{0}$ has been dropped, there is no uniform part and, since the mixture is incompressible as a whole,

$$\boldsymbol{\nabla} \cdot \boldsymbol{u}_m = 0, \tag{71}$$

as is obvious from (60). This implies that the parallel component of the non-uniform part of $\boldsymbol{u}_m$ should be zero. The numerical results also indicate that the cosine coefficient of the non-uniform parts for the force problem, and the sine coefficients for torque and shear problems, are less than 10% relative to the non-zero coefficients at most. This is of the order of the statistical error which may be expected, and we therefore assume them to vanish. Upon retaining only the non-zero terms, in the notation of the preceding section, we then have

$$\langle \tilde{\boldsymbol{u}}_m^s(\boldsymbol{k}) \rangle_s = [u_m]_F^\perp \boldsymbol{W}_F^\perp, \tag{72}$$

$$\langle \tilde{\boldsymbol{u}}_m^c(\boldsymbol{k}) \rangle_s = [u_m]_T^\perp \boldsymbol{W}_T^\perp, \tag{73}$$

$$\langle \tilde{\boldsymbol{u}}_m^c(\boldsymbol{k}) \rangle_s = [u_m]_E^\perp \boldsymbol{W}_E^\perp, \tag{74}$$

from which

$$\begin{aligned} \langle \boldsymbol{u}_m - \boldsymbol{u}^\infty \rangle(\boldsymbol{x}) &= \epsilon \sin(\boldsymbol{k}\cdot\boldsymbol{x})\, [u_m]_F^\perp \boldsymbol{W}_F^\perp \\ &\quad + \epsilon \cos(\boldsymbol{k}\cdot\boldsymbol{x})\, [u_m]_T^\perp \boldsymbol{W}_T^\perp \\ &\quad + \epsilon \cos(\boldsymbol{k}\cdot\boldsymbol{x})\, [u_m]_E^\perp \boldsymbol{W}_E^\perp. \end{aligned} \tag{75}$$

The three parameters denoted by [ ] in the parameterizations (72) to (74) are the building blocks of the analysis of non-uniform suspensions given in the next section.

The angular velocity of the mixture, $\boldsymbol{\Omega}_m$, is

$$\boldsymbol{\Omega}_m = \frac{1}{2} \boldsymbol{\nabla} \times \boldsymbol{u}_m. \tag{76}$$

Substituting (75), we have

$$\begin{aligned} \langle \boldsymbol{\Omega}_m - \frac{1}{2}\boldsymbol{\nabla} \times \boldsymbol{u}^\infty \rangle(\boldsymbol{x}) &= \epsilon \cos(\boldsymbol{k}\cdot\boldsymbol{x})\, \frac{k}{2}\, [u_m]_F^\perp \boldsymbol{\omega}_F^\perp \\ &+ \epsilon \sin(\boldsymbol{k}\cdot\boldsymbol{x})\, \frac{k}{2}\, [u_m]_T^\perp \boldsymbol{\omega}_T^\perp \\ &- \epsilon \sin(\boldsymbol{k}\cdot\boldsymbol{x})\, \frac{k}{2}\, [u_m]_E^\perp \boldsymbol{\omega}_E^\perp \end{aligned} \tag{77}$$

2. Particle quantities

In order to calculate the average of the particle velocity $\boldsymbol{U}$, for each configuration, we find its Fourier coefficients $\tilde{\boldsymbol{U}}(\boldsymbol{0})$, $\tilde{\boldsymbol{U}}^c$, and $\tilde{\boldsymbol{U}}^s$ according to (23) and (24), and we average them over the configurations to find $\langle \tilde{\boldsymbol{U}}(\boldsymbol{0}) \rangle_0$, $\langle \tilde{\boldsymbol{U}}^c \rangle_s$, and $\langle \tilde{\boldsymbol{U}}^s \rangle_s$. From the numerical results, the uniform parts for the torque and shear problems, the cosine coefficient of the non-uniform part for the force problem, and the sine coefficients for the torque and shear problems vanish. Upon using parameterizations in the form (50), we have then

$$\begin{aligned} &\langle \boldsymbol{U} - \boldsymbol{U}^\infty \rangle^P(\boldsymbol{x}) = [U]_F^0\, \boldsymbol{W}_F \\ &+ \epsilon \sin(\boldsymbol{k}\cdot\boldsymbol{x}) \left([U]_F^\parallel \boldsymbol{W}_F^\parallel + [U]_F^\perp \boldsymbol{W}_F^\perp \right) \\ &+ \epsilon \cos(\boldsymbol{k}\cdot\boldsymbol{x})\, [U]_T^\perp \boldsymbol{W}_T^\perp \\ &+ \epsilon \cos(\boldsymbol{k}\cdot\boldsymbol{x}) \left([U]_E^\parallel \boldsymbol{W}_E^\parallel + [U]_E^\perp \boldsymbol{W}_E^\perp \right). \end{aligned} \tag{78}$$

Similarly, for the particle angular velocity $\boldsymbol{\Omega}$, we have

$$\begin{aligned} \langle \boldsymbol{\Omega} - \boldsymbol{\Omega}^\infty \rangle^P(\boldsymbol{x}) &= [\Omega]_T^0\, \boldsymbol{W}_T \\ &\quad + \epsilon \cos(\boldsymbol{k}\cdot\boldsymbol{x})\, [\Omega]_F^\perp \boldsymbol{\omega}_F^\perp \\ &\quad + \epsilon \sin(\boldsymbol{k}\cdot\boldsymbol{x}) \left([\Omega]_T^\parallel \boldsymbol{\omega}_T^\parallel + [\Omega]_T^\perp \boldsymbol{\omega}_T^\perp \right) \\ &\quad + \epsilon \sin(\boldsymbol{k}\cdot\boldsymbol{x})\, [\Omega]_E^\perp \boldsymbol{\omega}_E^\perp. \end{aligned} \tag{79}$$

Note that $\langle \boldsymbol{U}^\infty \rangle^P$ $\langle \boldsymbol{\Omega}^\infty \rangle^P$ are the particle averages of the moments of the imposed velocity defined in (53) and in (54).

3. Slip velocities

The translational slip velocity $\langle \boldsymbol{u}_\Delta \rangle$ is the average translational velocity of the particles relative to the mixture:

$$\langle \boldsymbol{u}_\Delta \rangle = \langle \boldsymbol{U} - \boldsymbol{U}^\infty \rangle^P - \langle \boldsymbol{u}_m - \boldsymbol{u}^\infty \rangle. \tag{80}$$

Upon inserting the expression (55) for $\boldsymbol{U}^\infty(\alpha)$ into (22) and then into (25) to calculate $\langle \boldsymbol{U}^\infty \rangle^P$, because of the presence of the factor $\delta(\boldsymbol{x} - \boldsymbol{x}^\alpha)$, we simply find

$$\langle \boldsymbol{U}^\infty \rangle^P = \left(1 + \frac{a^2}{6} \nabla^2 \right) \boldsymbol{u}^\infty(\boldsymbol{x}). \tag{81}$$

Furthermore, in the three cases studied in this paper, $\boldsymbol{u}^\infty(\boldsymbol{x})$ is either a constant or a linear function of $\boldsymbol{x}$ so that the second term can be dropped with the result

$$\langle \boldsymbol{u}_\Delta \rangle = \langle \boldsymbol{U} \rangle^P - \langle \boldsymbol{u}_m \rangle. \tag{82}$$

From the parameterizations of the particle velocity in (78) and of the mixture velocity in (75), we have

$$\begin{aligned} &\langle \boldsymbol{u}_\Delta \rangle(\boldsymbol{x}) = [u_\Delta]_F^0\, \boldsymbol{W}_F \\ &+ \epsilon \sin(\boldsymbol{k}\cdot\boldsymbol{x}) \left([u_\Delta]_F^\parallel \boldsymbol{W}_F^\parallel + [u_\Delta]_F^\perp \boldsymbol{W}_F^\perp \right) \\ &+ \epsilon \cos(\boldsymbol{k}\cdot\boldsymbol{x})\, [u_\Delta]_T^\perp \boldsymbol{W}_T^\perp \\ &+ \epsilon \cos(\boldsymbol{k}\cdot\boldsymbol{x}) \left([u_\Delta]_E^\parallel \boldsymbol{W}_E^\parallel + [u_\Delta]_E^\perp \boldsymbol{W}_E^\perp \right), \end{aligned} \tag{83}$$

where

$$[u_\Delta]^0_F = [U]^0_F\,, \tag{84}$$
$$[u_\Delta]^\parallel_F = [U]^\parallel_F\,, \tag{85}$$
$$[u_\Delta]^\perp_F = [U]^\perp_F - [u_m]^\perp_F\,, \tag{86}$$
$$[u_\Delta]^\perp_T = [U]^\perp_T - [u_m]^\perp_T\,, \tag{87}$$
$$[u_\Delta]^\parallel_E = [U]^\parallel_E\,, \tag{88}$$
$$[u_\Delta]^\perp_E = [U]^\perp_E - [u_m]^\perp_E\,. \tag{89}$$

The slip angular velocity $\boldsymbol{\Omega}_\Delta$ is defined similarly by

$$\langle \boldsymbol{\Omega}_\Delta \rangle = \langle \boldsymbol{\Omega} - \boldsymbol{\Omega}^\infty \rangle^P - \langle \boldsymbol{\Omega}_m - \frac{1}{2}\boldsymbol{\nabla} \times \boldsymbol{u}^\infty \rangle. \tag{90}$$

which, in the present case, by the same argument as before, becomes

$$\langle \boldsymbol{\Omega}_\Delta \rangle = \langle \boldsymbol{\Omega} \rangle^P - \langle \boldsymbol{\Omega}_m \rangle. \tag{91}$$

From the parameterizations of the angular particle velocity in (79) and of the angular mixture velocity in (77),

$$\begin{aligned}\langle \boldsymbol{\Omega}_\Delta \rangle(\boldsymbol{x}) \;=\; & [\Omega_\Delta]^0_T\, \boldsymbol{W}_T \\ & + \epsilon \cos(\boldsymbol{k}\cdot\boldsymbol{x})\, [\Omega_\Delta]^\perp_F\, \boldsymbol{\omega}^\perp_F \\ & + \epsilon \sin(\boldsymbol{k}\cdot\boldsymbol{x}) \left([\Omega_\Delta]^\parallel_T\, \boldsymbol{\omega}^\parallel_T + [\Omega_\Delta]^\perp_T\, \boldsymbol{\omega}^\perp_T \right) \\ & + \epsilon \sin(\boldsymbol{k}\cdot\boldsymbol{x})\, [\Omega_\Delta]^\perp_E\, \boldsymbol{\omega}^\perp_E,\end{aligned} \tag{92}$$

where

$$[\Omega_\Delta]^\perp_F = [\Omega]^\perp_F - \frac{k}{2}\,[u_m]^\perp_F\,, \tag{93}$$
$$[\Omega_\Delta]^0_T = [\Omega]^0_T\,, \tag{94}$$
$$[\Omega_\Delta]^\parallel_T = [\Omega]^\parallel_T\,, \tag{95}$$
$$[\Omega_\Delta]^\perp_T = [\Omega]^\perp_T - \frac{k}{2}\,[u_m]^\perp_T\,, \tag{96}$$
$$[\Omega_\Delta]^\perp_E = [\Omega]^\perp_E + \frac{k}{2}\,[u_m]^\perp_E\,. \tag{97}$$

V. RESULTS

We now present and discuss the results of the multiparticle simulations in the light of the framework established in the previous sections. We focus on the the slip velocity $\langle \boldsymbol{u}_\Delta \rangle$, the mixture velocity $\langle \boldsymbol{u}_m - \boldsymbol{u}^\infty \rangle$, and the slip angular velocity $\langle \boldsymbol{\Omega}_\Delta \rangle$. These quantities are parameterized as in (83), (75), and (92), respectively, and we will examine the numerical coefficients in these parameterizations denoted by [ ]. These coefficients depend on both the wave vector k and the volume fraction ϕ.

A. Velocities for the force problem

We start by considering the velocities in the force problem.

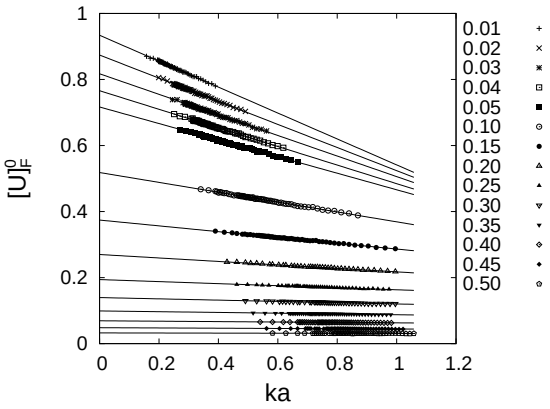

FIG. 5: Uniform part $[U]^0_F$ of the particle velocity for the force problem as a function of k. The points are the numerically calculated ensemble averages and the lines least-squares fits. For this problem, $[U]^0_F$ equals the uniform part $[u_\Delta]^0_F$ of the slip velocity.

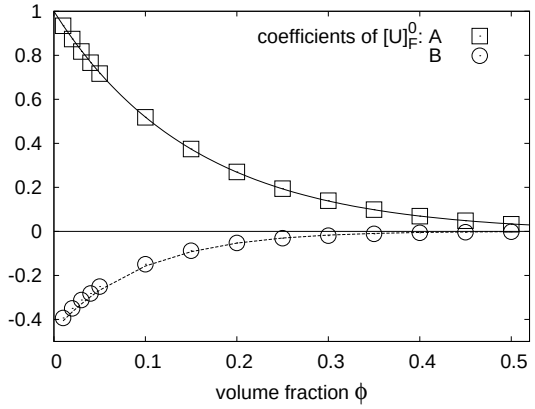

FIG. 6: Coefficients A and B of the linear fit (98) to $[U]^0_F$ as functions of the volume fraction ϕ. A coincides with the hindrance function $U(\phi)$ in (99) and B is the effect of the periodicity of the system. Solid and dashed lines are the fitting (100) for A and the model (101) for B, respectively.

Figure 5 shows, for different volume fractions between 1% and 50%, straight-line fits to the coefficients of the parameterization of the uniform part of $\langle \boldsymbol{U} - \boldsymbol{U}^\infty \rangle^P$:

$$[U]^0_F(k,\phi) = A^{[U]^0_F} + kB^{[U]^0_F}. \tag{98}$$

The fitting is done by least squares. The error with which (98) approximates the numerical results is smaller than the symbols used to graph $A^{[U]^0_F}$ and $B^{[U]^0_F}$ in Fig. 6. The constant term $A^{[U]^0_F}$ is the hindrance function for sedimentation, $U(\phi)$:

$$A^{[U]^0_F} = \lim_{k\to 0} [U]^0_F = U(\phi). \tag{99}$$

Therefore, $A^{[U]^0_F}$ is the sedimentation velocity extrapolated to infinite cell size. As Fig. 6 shows, it is well fitted

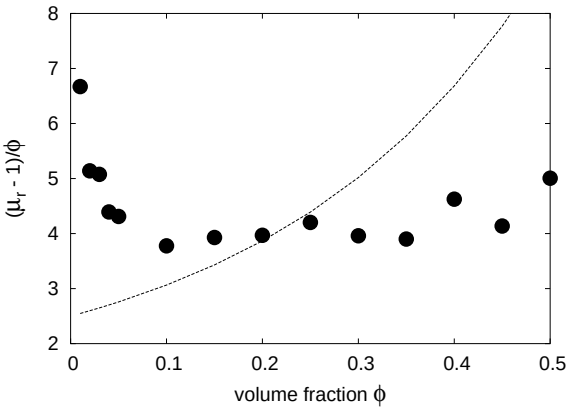

FIG. 7: Comparison of $(\mu_r - 1)/\phi$ as calculated directly by averaging the stresslets for the uniform shear problem (line) and from the suggestion (101) of Ref. 31.

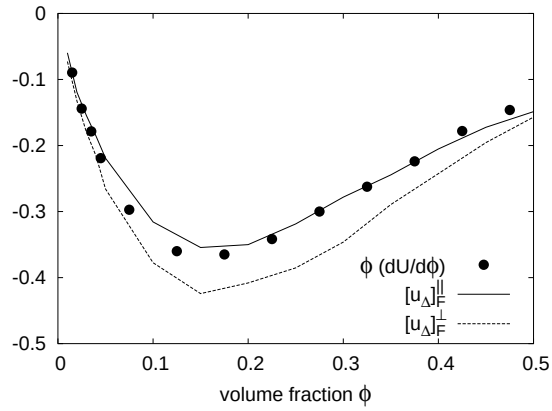

FIG. 8: Comparison among $\phi\,(\mathrm{d}U/\mathrm{d}\phi)$, $[u_\Delta]_F^{\parallel}$, and $[u_\Delta]_F^{\perp}$ for a non-uniform suspension. The three quantities should coincide if the relation between the force on the particles and the slip velocity did not contain a Faxén-type correction.

by

$$U(\phi) = (1-\phi)^{6.55-3.4\phi}. \tag{100}$$

Note that our numerical solution is affected by the truncation of the multipole expansion because we solve the many-body problems including multipoles only up to the fifth order.

The coefficient $B(\phi)$ reflects the effect of the periodicity[10,15,31] which arises from the difference between the sedimentation velocities of random and regular arrays.[41] Several heuristic arguments have been proposed leading to a relation between B and μ_r, the effective viscosity of the suspension normalized by the fluid viscosity. Mo and Sangani[31] propose a relation which, in our notation, is

$$B^{[U]_F^0} = -\frac{1.7601}{(6\pi^2)^{1/3}}\frac{S(0)}{\mu_r}, \tag{101}$$

in which $S(0)$ is the structure factor for $k = 0$. This is also plotted by the dashed line in Fig. 6, where μ_r is evaluated from the uniform shear problem as the average stresslets in the standard way.[10,15,31] Although the model (101) captures the qualitative behavior of B, there is a significant difference between $(\mu_r - 1)/\phi$ as calculated directly and the value deduced from (101). To better illustrate this difference, Fig. 7 shows $(\mu_r - 1)/\phi$ calculated from (101), which, in the dilute limit, should tend to the Einstein coefficient 5/2 multiplying the $O(\phi)$ term of μ_r. A similar difference can be observed in Fig. 6 of our previous paper.[27] These results suggest that the relationship between μ_r and $B^{[U]_F^0}$ is more complex than (101) would imply.

The coefficients for the non-uniform parts of $\langle \boldsymbol{U} - \boldsymbol{U}^\infty\rangle^P$ and $\langle \boldsymbol{u}_m - \boldsymbol{u}^\infty\rangle$ can be fitted as

$$[U]_F^{\parallel} = A^{[U]_F^{\parallel}} + kB^{[U]_F^{\parallel}}, \tag{102}$$

$$[U]_F^{\perp} = \frac{1}{k^2}D^{[U]_F^{\perp}} + A^{[U]_F^{\perp}} + kB^{[U]_F^{\perp}}, \tag{103}$$

$$[u_m]_F^{\perp} = \frac{1}{k^2}D^{[u_m]_F^{\perp}} + A^{[u_m]_F^{\perp}} + kB^{[u_m]_F^{\perp}}. \tag{104}$$

For $k \to 0$, we encounter in the terms D of the perpendicular components the same divergence found in Ref. 27. This arises from the lowest order multipole in (60). As noted in Ref. 27, this divergence is physical in that it is due to the fact that, as $k \to 0$, the width (and therefore the weight) of the heavier and lighter bands of mixture increases, while the shear force which retards their fall does not. These two diverging terms are found to be equal within our numerical accuracy and therefore cancel upon forming the perpendicular component of the slip velocity, which is therefore given by

$$[u_\Delta]_F^{\perp} = A^{[u_\Delta]_F^{\perp}} + kB^{[u_\Delta]_F^{\perp}}. \tag{105}$$

The coefficients $A^{[u_\Delta]_F^{\perp}}$ and $B^{[u_\Delta]_F^{\perp}}$ are calculated by fitting a linear k-dependence to the difference (86).

In order to understand these results, the simplest hypothesis is that the slip velocity is given by the hindrance function evaluated at the local volume fraction. For the linear sinusoidal non-uniformity (27), we would then have

$$U(\phi) = U(\phi_0) + \phi_0\frac{\mathrm{d}U}{\mathrm{d}\phi}\epsilon\sin\left(\boldsymbol{k}\cdot\boldsymbol{x}\right). \tag{106}$$

Figure 8 shows $[u_\Delta]_F^{\parallel}$, $[u_\Delta]_F^{\perp}$, and $\phi\,(\mathrm{d}U/\mathrm{d}\phi)$, where the derivative of the hindrance function is evaluated by numerical differentiation of the results for $[u_\Delta]_F^0$. We see that the simple hypothesis works quite well for the parallel component, but not for the perpendicular one.

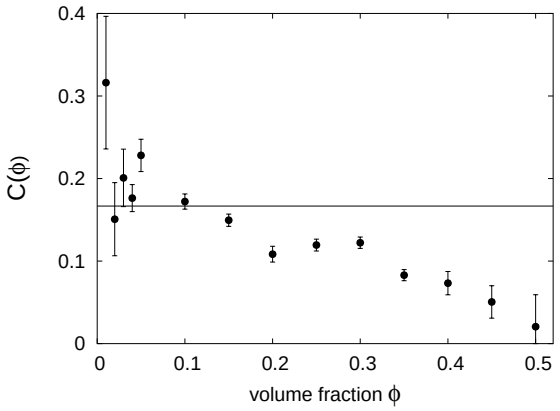

FIG. 9: Coefficient $C(\phi)$ of the Faxén-type correction of the relation between force on the particles and slip velocity defined in (109). The line is the dilute-limit value 1/6. The fitting error bars are also shown.

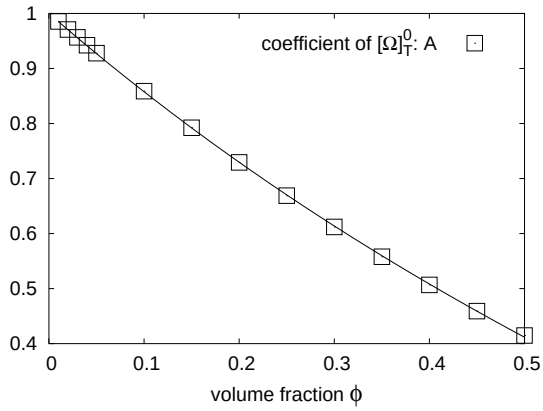

FIG. 10: Hindrance function for rotation $A = \Omega(\phi)$ as a function of the volume fraction.

To address this difference, it is useful to remember Faxén's law for a single particle

$$\frac{\boldsymbol{F}^\alpha}{6\pi\mu a} = \boldsymbol{U}^\alpha - \left(1 + \frac{a^2}{6}\nabla^2\right)\boldsymbol{u}'\left(\boldsymbol{x}^\alpha\right), \tag{107}$$

where $\boldsymbol{u}'$ is the velocity field except for the contribution of the particle α. It is reasonable to expect a similar contribution in the present case. Since the mixture velocity $\boldsymbol{u}_m$ only has a perpendicular component, this contribution would vanish for the parallel one, which would account for the good fit of $[u_\Delta]^\parallel_F$ and (106).

We thus introduce a coefficient $C(\phi;k)$ by

$$U(\phi)\,\frac{\boldsymbol{F}_0}{6\pi\mu a} = \langle\boldsymbol{u}_\Delta\rangle - C(\phi;k)a^2\nabla^2\langle\boldsymbol{u}_m\rangle. \tag{108}$$

Physically, this equation represents an extension of Faxén's law (107) and of the dilute-limit theory by Geigenmüller and Mazur[42] to finite volume fraction. Extrapolating to large system size, from the previous results, we find

$$C(\phi) = \lim_{k\to 0}\frac{1}{k^2a^2\,[u_m]^\perp_F}\left([u_\Delta]^\parallel_F - [u_\Delta]^\perp_F\right). \tag{109}$$

Figure 9 shows the values of $C(\phi)$ calculated from this expression together with the reference value 1/6 suggested by Faxén's law (107). The bars indicate the fitting error of the least-squares procedure. Convergence is poor at low volume fractions where, due to the increased available phase-space volume, a large number of configurations is necessary for a good statistical averaging. At high volume fractions, the error is possibly related to the truncation of the multipole expansion. Nevertheless, we find a general consistency between our results and (107). It should be stressed that, since $C(\phi)$ is independent of k, by superposition and linearity, the result (108) holds not only for the special form (26) of $n(\boldsymbol{x})$ but, to order $(a/L)^2$, for any other weak non-uniformity as well.

The Faxén term in Eq. (108) was also studied in our previous paper,[22] where Fig. 10 is, in the present notation, $C(\phi)/U(\phi)$. The present results are consistent with the earlier ones except for the last point in the latter corresponding to $\phi = 0.35$. Due to the smaller number of simulations conducted for that earlier study, it is likely that that point is in error.

In conclusion, we have found that the averages of the slip velocity are given by

$$[u_\Delta]^0_F = U(\phi), \tag{110}$$

$$[u_\Delta]^\parallel_F = \phi\frac{\mathrm{d}U}{\mathrm{d}\phi}, \tag{111}$$

$$[u_\Delta]^\perp_F + C(\phi)k^2[u_m]^\perp_F = \phi\frac{\mathrm{d}U}{\mathrm{d}\phi}. \tag{112}$$

Feuillebois[20] studied the sedimentation of a dilute suspension exhibiting a sinusoidal as well as a step-like non-uniformity taking only two-body interactions into account. In the dilute limit, his results are consistent with the present ones.[27]

B. Angular velocities for the torque problem

For fixed ϕ, the uniform part of the particle angular velocity has essentially no k dependence and is well fitted by a constant:

$$[\Omega]^0_T(k,\phi) = A^{[\Omega]^0_T} = \Omega(\phi), \tag{113}$$

where $\Omega(\phi)$ is the hindrance function for the torque problem. Figure 10 shows $A^{[\Omega]^0_T}$, which is well fitted by

$$\Omega(\phi) = (1-\phi)^{1.50-0.41\phi}. \tag{114}$$

The non-uniform parts of Ω can be fitted by

$$[\Omega]^\parallel_T = A^{[\Omega]^\parallel_T} + k^2C^{[\Omega]^\parallel_T}, \tag{115}$$

$$[\Omega]^\perp_T = A^{[\Omega]^\perp_T} + k^2C^{[\Omega]^\perp_T}. \tag{116}$$

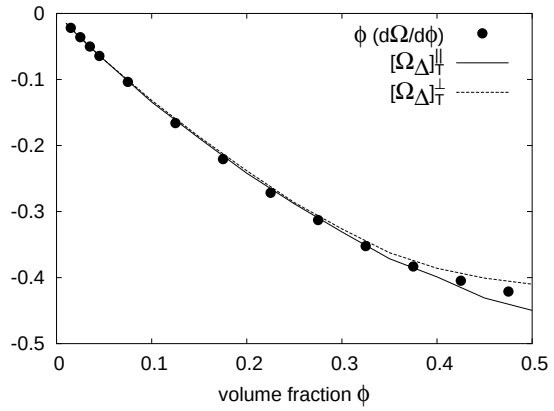

FIG. 11: Comparison among $\phi\,(\mathrm{d}\Omega/\mathrm{d}\phi)$, $[\Omega_\Delta]_T^{\parallel}$, and $[\Omega_\Delta]_T^{\perp}$ in a non-uniform suspension. The very close similarity among the three quantities implies that the mean torque is directly related to the slip angular velocity without a Faxén-type correction.

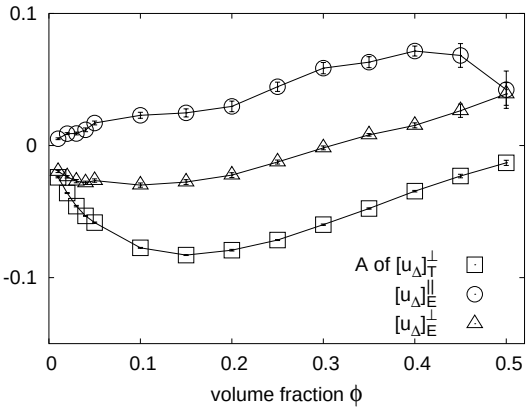

FIG. 12: Coefficient A of the linear term in k in the fits of the numerical results for $[u_\Delta]_T^{\perp}$, $[u_\Delta]_E^{\parallel}$, and $[u_\Delta]_E^{\perp}$ for the non-uniform case. Note that, while these quantities would all vanish for a uniform suspension, they are clearly non-zero in the presence of a non-uniformity. The fitting error bars are also shown.

As expected, there is no diverging term here. The mixture contribution to the angular velocity Ω_m is

$$[\Omega_m]_T^{\perp} = \frac{k}{2}\,[u_m]_T^{\perp} = \frac{k^2}{2}\left(\frac{D^{[u_m]_T^{\perp}}}{k^2} + A^{[u_m]_T^{\perp}}\right). \quad (117)$$

The leading terms of Ω and Ω_m are now different and no cancellation occurs in the calculation of the slip angular velocity, which is

$$[\Omega_\Delta]_T^{\perp} = A^{[\Omega_\Delta]_T^{\perp}} + k^2 C^{[\Omega_\Delta]_T^{\perp}}. \quad (118)$$

If the local slip angular velocity were only dependent on the local value of the rotational hindrance function, one would expect that

$$\Omega(\phi)\,\boldsymbol{T}_0 \;=\; 8\pi\mu a^3\langle\boldsymbol{\Omega}_\Delta\rangle \quad (119)$$

where

$$\Omega(\phi) \;=\; \Omega(\phi_0) + \phi_0\frac{d\Omega}{d\phi}\epsilon\,\sin\left(\boldsymbol{k}\cdot\boldsymbol{x}\right) \quad (120)$$

so that

$$[\Omega_\Delta]_T^{0} \;=\; \Omega(\phi), \quad (121)$$

$$[\Omega_\Delta]_T^{\parallel} \;=\; [\Omega_\Delta]_T^{\perp} = \phi\frac{\mathrm{d}\Omega}{\mathrm{d}\phi}, \quad (122)$$

which is tested numerically in Fig. 11. Unlike the force case, the numerical results evidently support the conjecture (119), which conforms with the conventional Faxén law for the torque on a single particle. The same argument presented before in connection with (108) can be repeated to conclude that (119) holds to order $(a/L)^2$ for any weak spatial non-uniformity.

C. Further examples of the effect of non-uniformity

For uniform suspensions, the slip velocity under an applied torque, the slip angular velocity for sedimentation, and both slip an slip-angular velocities for an imposed shear all vanish. The situation is different in the presence of spatial non-uniformities as we now show.

The computed average velocities for the torque problem can be fitted as

$$[U]_T^{\perp} \;=\; k\left(\frac{1}{k^2}D^{[U]_T^{\perp}} + A^{[U]_T^{\perp}}\right), \quad (123)$$

$$[u_m]_T^{\perp} \;=\; k\left(\frac{1}{k^2}D^{[u_m]_T^{\perp}} + A^{[u_m]_T^{\perp}}\right). \quad (124)$$

It is shown analytically in 27 that

$$\lim_{\phi\to 0} D^{[u_m]_T^{\perp}} = 3\phi. \quad (125)$$

Similarly to the force problem, the diverging terms of U and u_m are identical, and the leading term of the slip velocity is $O(k)$:

$$[u_\Delta]_T^{\perp} = kA^{[u_\Delta]_T^{\perp}}. \quad (126)$$

The coefficient $A^{[u_\Delta]_T^{\perp}}$ is shown by the squares in Fig. 12. The error bars inscribed in the symbols give an idea of the fitting error for this quantity. $A^{[u_\Delta]_T^{\perp}}$ is found to be rather small, but systematically non-zero.

For the shear problem, the parallel component of U can be fitted as

$$[U]_E^{\parallel} = kA^{[U]_E^{\parallel}}, \quad (127)$$

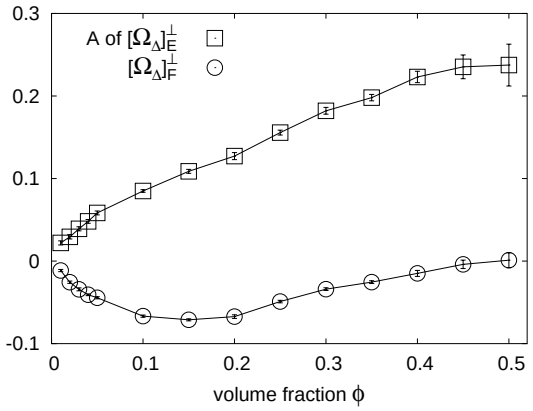

FIG. 13: Coefficient A of the linear term in k in the fits of the numerical results for $[\Omega_\Delta]^\perp_F$ and $[\Omega_\Delta]^\perp_E$ for the non-uniform case. While these quantities would all vanish for a uniform suspension, they are clearly non-zero in the presence of a non-uniformity. The fitting error bars are also shown.

and the perpendicular components of U and u_m as

$$[U]^\perp_E \;=\; k\left(\frac{1}{k^2}D^{[U]^\perp_E} + A^{[U]^\perp_E}\right), \tag{128}$$

$$[u_m]^\perp_E \;=\; k\left(\frac{1}{k^2}D^{[u_m]^\perp_E} + A^{[u_m]^\perp_E}\right), \tag{129}$$

where, for $D^{[u_m]^\perp_E}$ Ref. 27, shows that

$$\lim_{\phi\to 0} D^{[u_m]^\perp_E} = 5\phi. \tag{130}$$

The diverging terms again cancel upon forming the slip velocity and the leading term of this quantity is $O(k)$:

$$[u_\Delta]^\perp_E = kA^{[u_\Delta]^\perp_E}. \tag{131}$$

The A coefficients of the parallel and perpendicular components are also shown in Fig. 12 by the circles and triangles, respectively. The fitting error bars are inscribed in the symbols. Again, both of these quantities are clearly non-zero.

The average angular velocity coefficients in the force problem can be fitted as

$$[\Omega]^\perp_F \;=\; k\left(\frac{D^{[\Omega]^\perp_F}}{k^2} + A^{[\Omega]^\perp_F} + kB^{[\Omega]^\perp_F}\right), \tag{132}$$

$$[\Omega_m]^\perp_F \;=\; \frac{k}{2}\left(\frac{D^{[u_m]^\perp_F}}{k^2} + A^{[u_m]^\perp_F} + kB^{[u_m]^\perp_F}\right), \tag{133}$$

where we have diverging terms which, again, are equal, so that the leading order of the slip angular velocity is $O(k)$:

$$[\Omega_\Delta]^\perp_F = k\left(A^{[\Omega_\Delta]^\perp_F} + kB^{[\Omega_\Delta]^\perp_F}\right). \tag{134}$$

The circles in Fig. 13 shows $A^{[\Omega_\Delta]^\perp_F}$ with the fitting error bars.

The corresponding results for the problem take the form

$$[\Omega]^\perp_E \;=\; k^2\left(\frac{D^{[\Omega]^\perp_F}}{k^2} + A^{[\Omega]^\perp_F}\right), \tag{135}$$

$$[\Omega_m]^\perp_E \;=\; -\frac{k}{2}\left(\frac{D^{[u_m]^\perp_E}}{k^2} + A^{[u_m]^\perp_E}\right), \tag{136}$$

with identical diverging terms so that the leading order of the slip angular velocity is $O(k^2)$:

$$[\Omega_\Delta]^\perp_E = k^2 A^{[\Omega_\Delta]^\perp_E}. \tag{137}$$

Figure 13 shows this A coefficient with the fitting error bars.

These results show that, for non-uniform suspensions, the slip velocity $\langle \boldsymbol{u}_\Delta\rangle$ is non-zero even when no force acts on the particles, and the slip angular velocity $\langle \boldsymbol{\Omega}_\Delta\rangle$ is non-zero even in the absence of torques. This behavior is quite different from that encountered in the case of uniform suspensions and it suggests that uniform-suspension simulations can only give a partial view of the general behavior of a suspension. In particular, the characterization of non-uniform suspensions requires the introduction of additional "effective properties" (e.g., the Faxén coefficient) with respect to those sufficient to describe a uniform suspension. This issue has been partially addressed in Ref. 22 and will be pursued further in future publications.

VI. CONCLUSIONS

In the first part of this paper we have shown how averages corresponding to a spatially non-uniform statistical ensemble can be calculated on the basis of a uniform one. The method consists in attributing to each realization of the uniform ensemble a suitable weight, which is constructed explicitly starting from an arbitrarily prescribed macroscopic particle number density distribution.

We have applied this general theory to the simple case of a weak sinusoidal non-uniformity of the number density distribution of equal spheres in a viscous suspension for three mobility problems: sedimentation, applied torque, and imposed bulk shear flow. In spite of the special form of the non-uniformity, we have shown that the results are valid in general to second order in the ratio $(a/L)^2$, where a is the particle radius and L the macroscopic length scale.

We have found that, in a non-uniforms suspension, the average slip angular velocity, i.e. the relative angular velocity between the particles and the mixture, can be calculated by simply evaluating the hindrance function for rotation in correspondence of the local concentration, as in Eq. (119):

$$\langle \boldsymbol{\Omega}\rangle^P - \frac{1}{2}\boldsymbol{\nabla}\times\langle \boldsymbol{u}_m\rangle \;=\; \Omega(\phi)\,\frac{\boldsymbol{T}_0}{8\pi\mu a^3}\,, \tag{138}$$

where $\langle \boldsymbol{\Omega} \rangle^P$ is the average particle angular velocity, $\langle \boldsymbol{u}_m \rangle$ is the mixture volumetric flux, $\Omega(\phi)$ is the hindrance function for rotation shown in Fig. 10 and fitted as a function of ϕ by the expression (114), and $\boldsymbol{T}_0$ is the external torque applied to the particles.

An analogous relation for the translational slip velocity, however, does not hold. This quantity contains a finite-size correction proportional to $\nabla^2 \langle \boldsymbol{u}_m \rangle$, just as in the case of the familiar Faxén law for a single particle:

$$\langle \boldsymbol{U} \rangle^P - \langle \boldsymbol{u}_m \rangle \;=\; C(\phi) a^2 \nabla^2 \langle \boldsymbol{u}_m \rangle + U(\phi) \, \frac{\boldsymbol{F}_0}{6\pi\mu a} \tag{139}$$

in which $\langle \boldsymbol{U} \rangle^P$ is the mean particle translational velocity, $U(\phi)$ is the (translational) hindrance function, and $\boldsymbol{F}_0$ the external force applied to the particles. The dependence of the coefficient $C(\phi)$ on the volume fraction is shown in Fig. 9 and, within our numerical accuracy, is consistent with the usual value 1/6 as the particle volume fraction tends to zero.

The results (138) and (139) represent a generalization of the single-particle Faxén laws of Stokes flow to a spatially non-uniform suspension. The spatial non-uniformity that we have included in our study is limited to the particle number density, i.e. the one-body distribution function.

Acknowledgments

We wish to acknowledge the support by DOE grant DE-FG02-99ER14966.

APPENDIX A: DEFINITIONS FOR THE GENERALIZED MOBILITY PROBLEM

The generalized mobility equation (52) is derived from the integral equation (57).

The velocity and force moments are defined by

$$\mathscr{U}^{(n)}_{i,k\ldots}(\alpha) \;=\; \frac{1}{4\pi a^2} \int_{S^\alpha} dS(\boldsymbol{y}) \;\; (\boldsymbol{y} - \boldsymbol{x}^\alpha)^n_{k\ldots} \, v_i(\boldsymbol{y}) \tag{A1}$$

$$\mathscr{F}^{(n)}_{j,k\ldots}(\alpha) \;=\; -\int_{S^\alpha} dS(\boldsymbol{y}) \;\; (\boldsymbol{y} - \boldsymbol{x}^\alpha)^n_{k\ldots} \, f_j(\boldsymbol{y}). \tag{A2}$$

E^∞, and $\mathscr{U}^\infty$ are defined in terms of $\boldsymbol{u}^\infty(\boldsymbol{x})$ by

$$\begin{aligned} \mathsf{E}^\infty(\alpha) \;&=\; \frac{1}{4\pi a^2} \int_{S^\alpha} dS(\boldsymbol{y}) \;\; \frac{3}{2a^2} \left[(\boldsymbol{y} - \boldsymbol{x}^\alpha) \, \boldsymbol{u}^\infty(\boldsymbol{y}) \right. \\ &\qquad \left. + \boldsymbol{u}^\infty(\boldsymbol{y}) \;\; (\boldsymbol{y} - \boldsymbol{x}^\alpha) \right], \end{aligned} \tag{A3}$$

$$\mathscr{U}^{\infty\,(n)}(\alpha) \;=\; \frac{1}{4\pi a^2} \int_{S^\alpha} dS(\boldsymbol{y}) \;\; (\boldsymbol{y} - \boldsymbol{x}^\alpha)^n \, \boldsymbol{u}^\infty(\boldsymbol{y}). \tag{A4}$$

Corresponding expressions for $\boldsymbol{U}^\infty$, $\boldsymbol{\Omega}^\infty$ were presented earlier in (53) and (54).

If, as in the cases considered in this paper, the imposed flow is given by

$$\boldsymbol{u}^\infty(\boldsymbol{x}) = \boldsymbol{U}^0 + \boldsymbol{\Omega}^0 \times \boldsymbol{x} + \mathsf{E}^0 \cdot \boldsymbol{x}, \tag{A5}$$

then,

$$\boldsymbol{U}^\infty(\alpha) \;=\; \boldsymbol{U}^0 + \boldsymbol{\Omega}^0 \times \boldsymbol{x}^\alpha + \mathsf{E}^0 \cdot \boldsymbol{x}^\alpha, \tag{A6}$$

$$\boldsymbol{\Omega}^\infty(\alpha) \;=\; \boldsymbol{\Omega}^0, \tag{A7}$$

$$\mathsf{E}^\infty(\alpha) \;=\; \mathsf{E}^0, \tag{A8}$$

$$\mathscr{U}^\infty(\alpha) \;=\; 0. \tag{A9}$$

* Electronic address: ichiki@mailaps.org
† Electronic address: prosperetti@jhu.edu

[1] G. Batchelor, "Sedimentation in a dilute dispersion of spheres," J. Fluid Mech. **52**, 245 (1972).
[2] G. Batchelor and J. Green, "The determination of the bulk stress in a suspension of spherical particles to order c^2," J. Fluid Mech. **56**, 401 (1972).
[3] H. Brenner, "Suspension rheology in the presence of rotary Brownian motion and external couples: elongational flow of dilute suspensions," Chem. Eng. Sci. **27**, 1069 (1972).
[4] M. Zuzovsky, P. Adler, and H. Brenner, "Spatially periodic suspensions of convex particles in linear shear flows. III. Dilute arrays of spheres suspended in Newtonian fluids," Phys. Fluids **26**, 1714 (1983).
[5] H. Brenner, "Antisymmetric stress induced by the rigid-body rotation of dipolar suspensions," Int. J. Engng. Sci. **22**, 645 (1984).
[6] P. Mazur, "On the motion and Brownian motion of n spheres in a viscous fluid," Physica **110A**, 128 (1982).
[7] P. Mazur and W. van Saarlos, "Many-sphere hydrodynamic interactions and mobilities in a suspension," Physica **115A**, 21 (1982).
[8] J. Brady and G. Bossis, "Stokesian dynamics," Ann. Rev. Fluid Mech. **20**, 111 (1988).
[9] A. Sangani and A. Acrivos, "Slow flow through a periodic array of spheres," Int. J. Multiphase Flow **8**, 343 (1982).
[10] A. Ladd, "Hydrodynamic transport coefficients of random dispersions of hard spheres," J. Chem. Phys. **93**, 3484 (1990).
[11] A. Ladd, "Sedimentation of homogeneous suspensions of non-Brownian spheres," Phys. Fluids **9**, 491 (1997).
[12] A. Sangani and G. Mo, "An $O(N)$ algorithm for Stokes and Laplace interactions of particles," Phys. Fluids **8**, 1990 (1996).
[13] A. Sierou and J. Brady, "Accelerated Stokesian Dynamics simulations," J. Fluid Mech. **448**, 115 (2001).
[14] C. Chang and R. Powell, "The rheology of bimodal hard-sphere dispersions," Phys. Fluids **6**, 1628 (1994).
[15] R. Phillips, J. Brady, and G. Bossis, "Hydrodynamic transport properties of hard-sphere dispersions. I. Suspensions of freely mobile particles," Phys. Fluids **31**, 3462 (1988).
[16] J. Brady and L. Durlofsky, "The sedimentation rate of disordered suspensions," Phys. Fluids **31**, 717 (1988).
[17] P. Nott and J. Brady, "Pressure-driven flow of suspensions: simulation and theory," J. Fluid Mech. **275**, 157 (1994).
[18] J. Morris and J. Brady, "Pressure-driven flow of a suspension: buoyancy effects," Int. J. Multiphase Flow **24**, 105 (1998).
[19] M. Brenner, "Screening mechanisms in sedimentation," Phys. Fluids **11**, 754 (1999).
[20] F. Feuillebois, "Sedimentation in a dispersion with vertical inhomogeneities," J. Fluid Mech. **139**, 145 (1984).
[21] D. Lhuillier, "Ensemble averaging in slightly non-uniform suspensions," Eur. J. Mech. B/Fluids **11**, 649 (1992).
[22] M. Marchioro, M. Tanksley, W. Wang, and A. Prosperetti, "Flow of spatially non-uniform suspensions Part II: Systematic derivation of closure relations," Int. J. Multiphase Flow **27**, 237 (2001).
[23] D. Leighton and A. Acrivos, "The shear-induced migration of particles in concentrated suspensions," J. Fluid Mech. **181**, 415 (1987).
[24] M. Marchioro and A. Acrivos, "Shear-induced particle diffusivities from numerical simulations," J. Fluid Mech. **443**, 101 (2001).
[25] J. Luke, "Decay of velocity fluctuations in a stably stratified suspension," Phys. Fluids **12**, 1619 (2000).
[26] P. Segré, F. Liu, P. Umbanhovar, and D. Weitz, "An effective gravitational temperature for sedimentation," Nature **409**, 594 (2001).
[27] M. Marchioro, M. Tanksley, and A. Prosperetti, "Flow of spatially non-uniform suspensions. Part I: Phenomenology," Int. J. Multiphase Flow **26**, 783 (2000).
[28] W. Wang and A. Prosperetti, "Flow of spatially non-uniform suspensions. Part III: Closure relations for porous media and spinning particles," Int. J. Multiphase Flow **27**, 1627 (2001).
[29] M. Tanksley and A. Prosperetti, "Average pressure and velocity fields in non-uniform suspensions of spheres in Stokes flow," J. Eng. Math. **41**, 275 (2001).
[30] J. Brady, R. Phillips, J. Lester, and G. Bossis, "Dynamic simulation of hydrodynamically interacting suspensions," J. Fluid Mech. **195**, 257 (1988).
[31] G. Mo and A. Sangani, "A method for computing Stokes flow interactions among spherical objects and its application to suspensions of drops and porous particles," Phys. Fluids **6**, 1637 (1994).
[32] K. Ichiki, "Improvement of the Stokesian Dynamics method for systems with finite number of particles," J. Fluid Mech. **452**, 231 (2002).
[33] J. Happel and H. Brenner, *Low-Reynodls Number Hydrodynamics* (Pretice-Hall, Englewood Cliffs, 1965).
[34] S. Kim and S. Karrila, *Microhydrodynamics* (Butterworth-Heinemann, Boston, 1991).
[35] O. Ladyzhenskaya, *The Mathematical Theory of Viscous Incompressible Flow*, 2nd ed. (Gordon and Breach, New York, 1969).
[36] C. Pozrikidis, *Boundary Integral and Singularity Methods for Linearized Viscous Flow* (Cambridge U.P., Cambridge, 1992).
[37] H. Hasimoto, "On the periodic fundamental solutions of the Stokes equations and their application to viscous flow past a cubic array of spheres," J. Fluid Mech. **5**, 317 (1959).
[38] J. Percus and G. Yevick, "Analysis of classical statistical mechanics by means of collective coordinates," Phys. Rev. **110**, 1 (1958).
[39] M. S. Wertheim, "Exact solution of the Percus-Yevick integral equation for hard spheres," Phys. Rev. Lett. **10**, 321 (1963).
[40] E. Thiele, "Equation of state for hard spheres," J. Chem. Phys. **39**, 474 (1963).
[41] P. Saffman, "On the settling speed of free and fixed suspensions," Stud. Appl. Math. **52**, 115 (1973).
[42] U. Geigenmüller and P. Mazur, "Sedimentation of homogeneous suspensions in finite vessels," J. Stat. Phys. **53**, 137 (1988).